Controlling the interlayer-Dzyaloshinskii-Moriya-interaction by electrical currents

Fabian Kammerbauer,[†] Won-Young Choi,[†,‡] Frank Freimuth,[†,¶] Kyujoon Lee,[§] Robert Frömter,[†] Dong-Soo Han,[‡] Reinoud Lavrijsen,[‖] Henk J. M. Swagten,[‖] Yuriy Mokrousov,[†,¶] and Mathias Kläui*[,†]

†*Institute of Physics, Johannes Gutenberg-Universität Mainz, 55128 Mainz, Germany.*

‡*Center for Spintronics, Korea Institute of Science and Technology, 34141 Seoul, Republic of Korea.*

¶*Peter Grünberg Institut and Institute for Advanced Simulation, Forschungszentrum Jülich and JARA, 52425 Jülich, Germany.*

§*Division of display and semiconductor physics, Korea University, 30019 Sejong, Republic of Korea.*

‖*Department of Applied Physics, Institute for Photonic Integration, Eindhoven University of Technology, Eindhoven, The Netherlands.*

E-mail: klaeui@uni-mainz.de

Abstract

The recently discovered interlayer Dzyaloshinskii-Moriya interaction (IL-DMI) in multilayers with perpendicular magnetic anisotropy favors a canting of spins in the in-plane direction. It could thus stabilize intriguing spin textures such as Hopfions. A key requirement for nucleation is to control the IL-DMI. Therefore, we investigate the influence of an electric current on a synthetic antiferromagnet with growth-induced IL-DMI. The IL-DMI is quantified using out-of-plane hysteresis loops of the anomalous Hall effect while applying a static in-plane magnetic field at varied azimuthal angles. We observe a shift in the azimuthal dependence with increasing current, which is concluded to originate from the additional in-plane symmetry breaking introduced by the current flow. Fitting the angular dependence we demonstrate the presence of an additive current-induced term that linearly increases the IL-DMI in the direction of current flow. This opens the possibility to easily manipulate 3D spin textures by currents.

Keywords

interlayer Dzyaloshinskii-Moriya-interaction, synthetic antiferromagnet, magnetization switching, anomalous Hall effect, spintronics

The burgeoning field of 3D magnetism has introduced ways of bending and forming magnetic structures arbitrarily and fabricate complex shaped magnetic nanoparticles,[1] magnetic tubes[2] and others.[3,4] All these approaches have distinct features of manipulating the material itself towards shaping it also in the third dimension. Another approach towards 3D magnetism are 3D topological textures within the magnetic system itself.[3] These new 3D spin structures, such as hopfions,[5–8] offer advantages for future spintronic applications.[3,4] Compared to 2D spin structures, e.g. skyrmions stabilized by the Dzyaloshinskii-Moriya interaction (DMI),[9] it is more challenging to stabilize twisted spin configurations in the third dimension.[4] A recent first experimentally observed magnetic Hopfion has relied on a combination of strong DMI and the confinement in a nanodisk.[8]

Another route towards Hopfions is offered by the antisymmetric interlayer exchange interaction, which has been termed as RKKY-DMI or interlayer DMI (IL-DMI).[10–16] It favors spin canting between layers in the lateral direction and originates from an in-plane symmetry breaking. This allows for a highly sought-after tuning mechanism for 3D magnetic textures, which could stabilize such structures in magnetic multilayers without confinement. The absence of confinement opens the possibility to move or aggregate these structures. While it is interesting to study the internal dynamics under the application of fields or currents[17] a possibility to directly control the IL-DMI strength can additionally provide direct access to internal transformations between different 3D magnetic textures. This would allow for writing and deleting operations, which are necessary when employing the different magnetic textures as bits. Furthermore, the IL-DMI can allow for field-free switching as recent studies have shown.[15,16] This pure-electrical switching facilitated by the IL-DMI offers new possibilities for spintronic devices while the IL-DMI is relatively simply induced by an oblique sputtering technique[18] or a magnetic field during deposition.[11] Conventionally, the strength of both the DMI and the IL-DMI is set during sample growth. For DMI post-growth changes to its magnitude have been shown, while for the IL-DMI these are elusive so far. One possible option to influence the DMI is strain. It has been shown that strain can enhance the DMI[19,20] and be used to tune the diameter of skyrmions.[21] A technologically more easily accessible option is applying an electrical current, which is typically used to introduce spin-transfer torques and spin-orbit torques in many systems[22–25] and has been recently shown to directly influence the strength of the conventional DMI .[26–28] The benefit of this approach is the direct tuning parameter allowing one to locally change the DMI and therefore the spin structures can be dynamically controlled.

No post-growth tuning of the IL-DMI has been reported yet, while this is essential for functionalizing the effect. This study aims to investigate the effect of electrical currents on the IL-DMI, as a more direct and locally accessible tuning parameter compared to globally varying the in-plane symmetry breaking. To quantify the effect, we employ asymmetric

hysteresis-loop measurements, a technique previously introduced to confirm the presence of IL-DMI.[10] We use symmetry arguments to explain that stabilizing a chiral Néel-type state requires a gradient along the direction $(\boldsymbol{M}_1 \times \boldsymbol{M}_2) \times \boldsymbol{R}$, where $\boldsymbol{R}$ is the distance vector between the magnetizations $\boldsymbol{M}_1$ and $\boldsymbol{M}_2$ of the two layers. When this gradient is provided by an applied electric field, several mechanisms for tuning the IL-DMI become possible. One mechanism is the spin Hall effect, which extends the spin-current picture of equilibrium DMI[29,30] into the nonequilibrium regime.

The investigated sample is a synthetic antiferromagnet (SAF) of Ta(4)/Pt(4)/ Co(0.6)/Pt(0.7)/Ru(0.8)/Pt(0.5)/Co(1)/Pt(4) structure on Si/SiO_2 (layer thicknesses in nanometers). The two ferromagnetic (FM) layers, FM1 at the bottom and FM2 at the top, are antiferromagnetically coupled across the Ru layer via the Ruderman-Kittel-Kasuya-Yosida (RKKY) interaction. The in-plane symmetry breaking required for IL-DMI,[10,11] was introduced deliberately during film deposition via oblique sputtering. The film was then patterned into Hall bars. Details are provided in the experimental section.

To investigate the IL-DMI, the method devised by Han et al.[10] was employed. For the case of a sample with IL-DMI and perpendicular magnetic anisotropy (PMA) the magnetization switching by an out-of-plane (OOP) field sweep will be supported or hindered in the presence of an in-plane bias field, depending on its direction and the chirality of the DMI.[31] Similarly, in SAFs with PMA and IL-DMI, the magnetization switching is supported or hindered under application of an in-plane field depending on its azimuthal direction with respect to the in-plane symmetry breaking axis and the chirality introduced by the IL-DMI. This has been elaborated in depth by Han et al.[18] Hysteresis loops obtained by sweeping the OOP field were measured by the anomalous Hall effect (AHE) in the patterned Hall bars while applying an in-plane field of $H_{\mathrm{IN}} = 100$ mT along a selected direction. The AHE setup and two resulting hysteresis loops are shown in Fig. 1A-B). The switching fields of the two magnetic layers can be easily distinguished as the thicker FM2 gives rise to the higher jumps. In addition, the switching fields for the two distinct sweep directions up-to-down (U-D) and down-to-up

(D-U) of the hysteresis loops are considered separately. The concept of hindered and assisted switching due to IL-DMI is illustrated in two small sketches in Fig. 1B). For positive H_{IN} the IL-DMI assists D-U switching of the top layer FM2, as in the lower hysteresis branch IL-DMI and field act in the same direction, increasing the magnetization tilt. In contrast, the IL-DMI hinders U-D switching of FM2, as in the upper branch IL-DMI and field act in opposite directions, reducing the magnetization tilt. As the coupling strength of the investigated SAF is weak compared to typical antiferromagnets, the magnetization can be substantially tilted by moderate in-plane fields, as detailed in the supplementary material.

By varying ϕ in steps of 30° a full azimuthal dependence is obtained. This allows us to find the direction of the axis of the antisymmetric behaviour, which is the direction where the asymmetry between U-D and D-U switching fields is the largest, as shown in Fig. 1c) and d). There the antisymmetric axis points approximately along 300°. The presence of an antisymmetric axis indicates the presence of IL-DMI in this sample. An in-plane anisotropy as source for the broken symmetry can be ruled out due to the sample's polycrystalline nature averaging out over the large Hall-bar width. The latter does also not give rise to any significant in-plane shape anisotropy.

To quantify and compare the IL-DMI for several current densities we assume the IL-DMI to act as a bias field that shifts the hysteresis loop, as seen in Fig. 1b). This effect can be quantified by an IL-DMI field, which we name $H_{\mathrm{IL-DMI}}$. We define $H_{\mathrm{IL-DMI}}$ as the difference between the U-D and D-U switching fields divided by two.[13]

$$H_{\mathrm{IL-DMI}} = \frac{H_{\mathrm{SW,U-D}} + H_{\mathrm{SW,D-U}}}{2} \tag{1}$$

with $H_{\mathrm{SW,U-D}}$ and $H_{\mathrm{SW,D-U}}$ the switching fields for U-D and D-U switching, respectively, as illustrated in Fig. 1b). This description assumes that there are no other bias effects leading to asymmetric hysteresis loops, such as exchange bias[32,33] or biquadratic interlayer exchange interaction effects.[34] Fig. 2 presents the values of the $H_{\mathrm{IL-DMI}}$ field as function

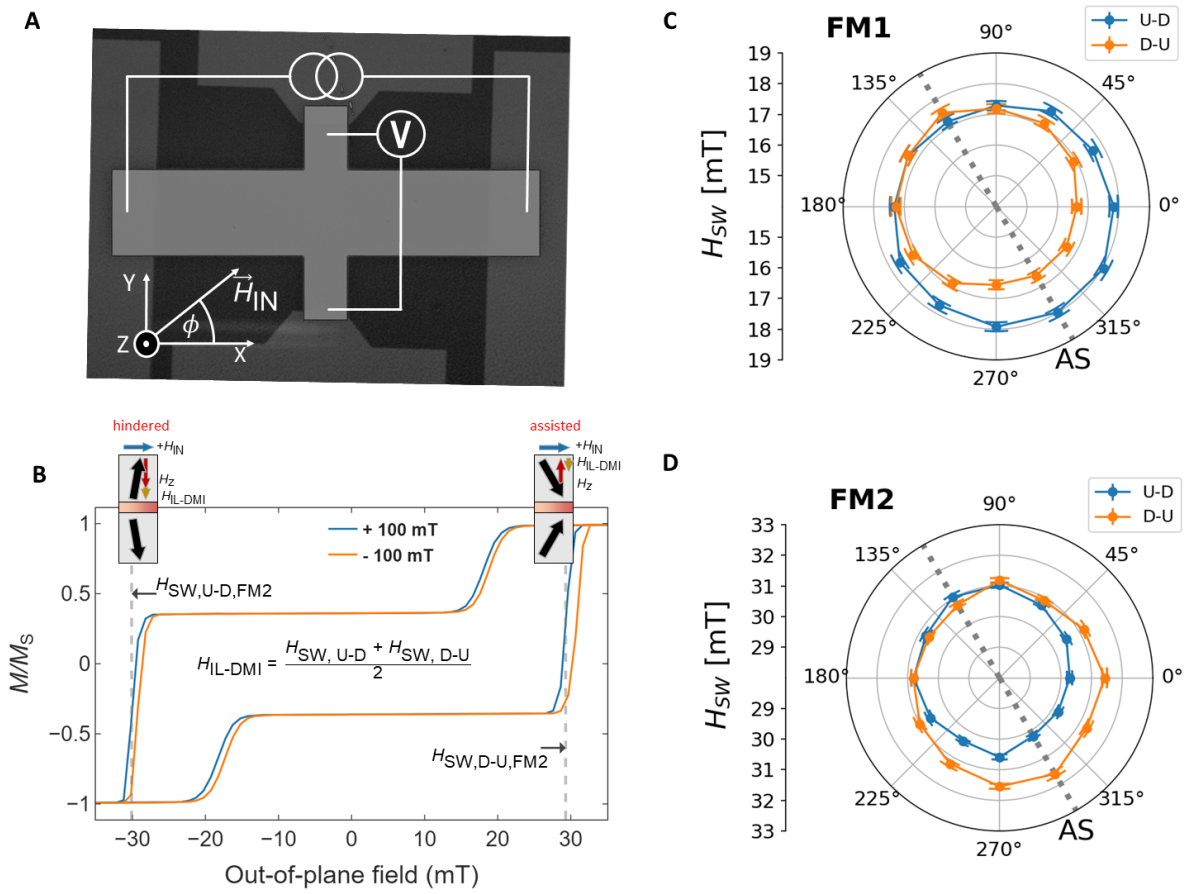

Figure 1: **Measurement setup and signature of the static IL-DMI.** (**A**) Hall-bar structure with indicated connections. For the anomalous Hall effect measurements a dc current along $+x$ direction is applied while sweeping the out-of-plane field in z-direction. Additionally, an in-plane field $\boldsymbol{H}_{\mathrm{IN}}$ of 100 mT is applied along an angle ϕ, with ϕ varying from 0° to 330° in 30° steps.(**B**) Magnetic hysteresis loops measured by anomalous Hall effect. Blue and orange curves display the hysteresis under the influence of a positive and negative in-plane field of 100 mT, respectively, that is aligned with the antisymmetric axis. The sketches illustrate the magnetization orientation for right-handed IL-DMI and positive in-plane magnetic field in two marked switching cases. H_{SW} is the superposition of $H_{\mathrm{IL-DMI}}$ and H_{Z}. The IL-DMI increases canting for U-D switching and decreases canting for D-U switching. $H_{\mathrm{IL-DMI}}$ is defined as the difference between the two switching fields. (**C**) and (**D**) show the switching field dependence on ϕ for FM1 and FM2, respectively, measured at a current density of 0.6×10^9 A/m^2. The antisymmetric axis (AS) is denoted by a grey dotted line.

of ϕ for the two different ferromagnetic layers for the lowest and highest applied current densities. The sinusoidal dependence on the angle is the fingerprint for the presence of an IL-DMI, as the latter is directly dependent on the angle between the applied field and the

in-plane inversion symmetry breaking, i.e., the antisymmetric axis. We can exclude any effect from biquadratic interlayer exchange, which would be isotropic in nature,[35] as also the DMI, which is symmetric in the field direction, i.e., $H_{\mathrm{SW}}(-\phi) = H_{\mathrm{SW}}(\phi)$.[31] Exchange bias can also be excluded as the investigated sample is a layered synthetic antiferromagnet. The coupling between the FM layers is weak in comparison to regular antiferromagnets and the magnetization can be canted by moderate external fields. This is discussed further in the supplementary material. Therefore, we can conclude that the IL-DMI is the origin of the shift of the hysteresis curves at low and high current densities.

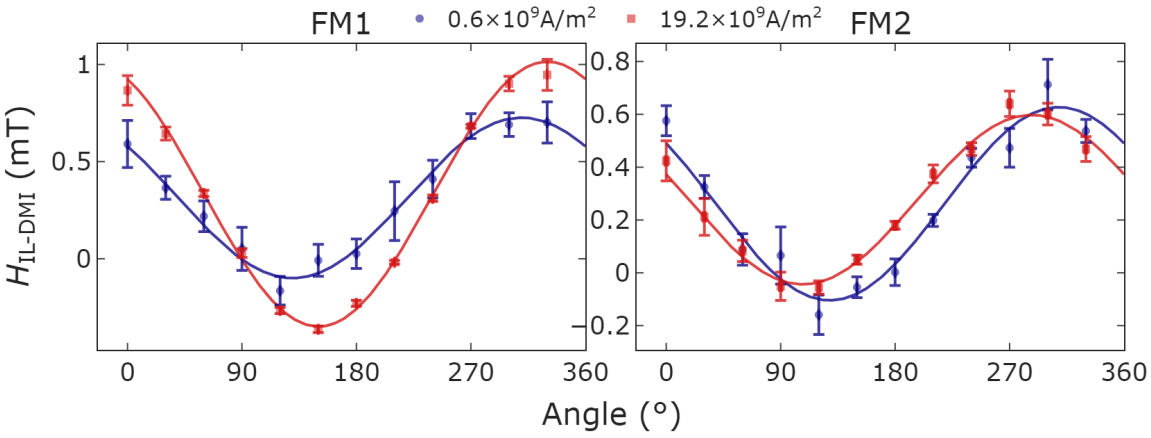

Figure 2: **The effect of current.** Azimuthal dependence of $H_{\mathrm{IL-DMI}}$ for the lowest current density at 0.6 $\times$ 10^9A/m^2 and a high current density at 19.2 $\times$ 10^9A/m^2, for FM1 on the left and FM2 on the right. The lines are sine fits to the data.

Next, we study the current dependence of the $H_{\mathrm{IL-DMI}}$ for FM1 and FM2 as shown in Fig. 2. Using a higher current, the $H_{\mathrm{IL-DMI}}$ amplitude changes, and the phase of the sine function fit is shifted. To analyze this functional behavior, we assume the contribution of the electrical current can be described by a superimposed cosine angular dependence that is of unknown strength but aligned with the direction of current flow. This results in a two-cosine model for $H_{\mathrm{IL-DMI}}$ where the first term is static, originating from the sample's intrinsic symmetry breaking, and the second term describes the current-induced effect. We

thus use the following model for a shared-parameter fit.

$$H_{\mathrm{IL-DMI}} = a_0 \cos(\phi - \phi_0) + a_j \cos(\phi - \phi_j) + b, \tag{2}$$

with ϕ, the angle of the applied field, ϕ_0 the angular direction of symmetry breaking defined by the sample growth, i.e., the maximum position of $H_{\mathrm{IL-DMI}}$ at zero applied current, ϕ_j the azimuthal direction of the current-induced IL-DMI, a_0 and a_j are the amplitudes and b is an offset. Note that the positive current direction is along 0° (see Fig. 1).

We assume the first term to be independent of current, thereby, ϕ_0 is fixed along the direction of the antisymmetric axis and determined by extrapolating cosine fits of the data to the zero current limit, which yields $301° \pm 5°$ for the case of FM1 and $311° \pm 6°$ for FM2.

Using Eq. (2) the whole data set of $H_{\mathrm{IL-DMI}}$ is fitted by a single multi-curve fit including all available current densities. a_0 and ϕ_j are expected to remain constant for all current densities, so they are set as shared parameters, while ϕ_0 is fixed to its extrapolated zero-current value. The a_j are not shared as they are expected to increase with current density. The resulting values of ϕ_j & a_0 are given in Table 1 and show that ϕ_j is indeed approximately 0°, i.e., aligned with the current direction. The trend of a_j with current density shows a linear increase, see Fig. 3, however, the slope is positive for FM1 and negative for FM2 as seen in the last column of Table 1. Furthermore, the effect is asymmetric in current, demonstrating that the effect is not induced by heating.

Table 1: **Fit results.** Shared parameters for all current densities obtained from fitting $H_{\mathrm{IL-DMI}}$ according to Eq. (2) and slope of the linear fits shown in Fig. 3. The initial value for ϕ_j is 0°.

layer	ϕ_j (°)	a_0 (mT)	slope (μT/10^9Am^{-2})
FM1	-3 ± 1	0.37 ± 0.01	16.8 ± 0.5
FM2	-6 ± 3	0.35 ± 0.01	-8.8 ± 0.8

The nature of this observation can be better understood when employing symmetry arguments. We may write the IL-DMI energy associated with the chiral state as $F =$

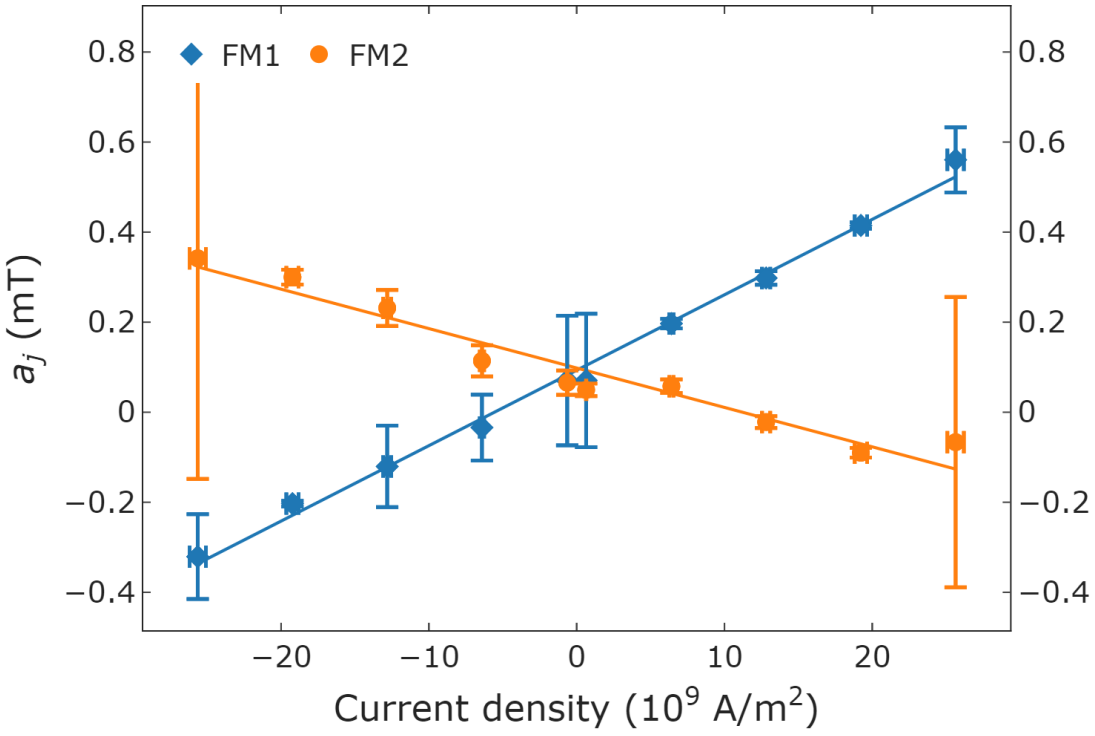

Figure 3: **Amplitude of current-induced DMI.** The current-induced contribution of the interlayer DMI a_j given by Eq. (2) as function of current density. The lines represent linear fits to the data up to a current density of $25.6 \times 10^9 \mathrm{A/m}^2$.

$(\boldsymbol{T}_2 - \boldsymbol{T}_1) \cdot (\boldsymbol{M}_1 \times \boldsymbol{M}_2)$, where $\boldsymbol{M}_1$ and $\boldsymbol{M}_2$ are the magnetizations in FM1 and FM2, respectively, and $\boldsymbol{T}_i$ is the contribution to the torque on $\boldsymbol{M}_i$ that stems from the IL-DMI (the total torque is zero in the stationary state). These torques $\boldsymbol{T}_i$ need to point into the direction of $\boldsymbol{M}_1 \times \boldsymbol{M}_2$ in order to produce a contribution to F (with $\boldsymbol{T}_1 \neq \boldsymbol{T}_2$). If the system contains a mirror plane that flips the sign of $\boldsymbol{M}_1 \times \boldsymbol{M}_2$, it therefore also flips the relevant component of $(\boldsymbol{T}_2 - \boldsymbol{T}_1)$ without changing the energy F, which is inconsistent with the DMI interaction that changes sign, when $\boldsymbol{M}_1 \times \boldsymbol{M}_2$ changes sign. This mirror plane may be eliminated by a material gradient or an applied electric current in the direction $(\boldsymbol{M}_1 \times \boldsymbol{M}_2) \times \boldsymbol{R}$, where $\boldsymbol{R}$ is the distance vector between the two ferromagnetic vectors. The injection of spin current from the SHE into the ferromagnetic layers may generate these torques $\boldsymbol{T}_2$ and $\boldsymbol{T}_1$. In this

case one may understand the IL-DMI also from the balance equation of the torques and it is not necessary to consider the energy F: The torque balance equations on FM1 and FM2 may be written as $-J(\boldsymbol{M}_1 \times \boldsymbol{M}_2) + \boldsymbol{T}_1 = 0$ and $-J(\boldsymbol{M}_2 \times \boldsymbol{M}_1) + \boldsymbol{T}_2 = 0$, where J is the exchange coupling. By summing these two equations one obtains a single equation: $2J(\boldsymbol{M}_1 \times \boldsymbol{M}_2) = \boldsymbol{T}_1 - \boldsymbol{T}_2$. Consequently, a chiral magnetic state characterized by the chirality $(\boldsymbol{M}_1 \times \boldsymbol{M}_2) \neq 0$ will occur when $\boldsymbol{T}_2 \neq \boldsymbol{T}_1$. In the samples considered it is likely that injection of spin current into the FM layers yields even different signs of $\boldsymbol{T}_2$ and $\boldsymbol{T}_1$. More details can be found in the supplementary material.

The change of the effect due to the current polarity shows that the effect does not arise from heating effects. To understand any effect heating may have on the sample, a continuous film of a similar sample system Ta(4)/Pt(4)/Co(0.6)/Pt(0.5)/Ru(0.8)/Pt(0.5)/Co(1)/Pt(4), was investigated in a cryostat as function of temperature. The effect on the IL-DMI field for temperatures varying between 200 K and 300 K is present but small, see Fig. 4. Given the small dependence of IL-DMI on temperature, as seen in Fig. 4, and the small effect of Joule heating, we simulated the Joule heating in the Hall bar using COMSOL multiphysics, similar to an approach used to estimate the heating in NiO/Pt systems.[36] The simulation yielded a Joule heating of about ≈ 5.5 K for a current density of $25.6 \times 10^9 \mathrm{A/m^2}$. If the effect was dominated by Joule heating, a decrease in $H_{\mathrm{IL-DMI}}$ with current should have been observed, which is not the case as shown in Fig. 2. Therefore, we can deduce that Joule heating plays a negligible role in the magnitude of the IL-DMI in our sample. Current-induced Oersted fields cannot explain the observed results for current-induced IL-DMI as neither the out-of-plane nor in-plane component can account for the opposite behavior of the two distinct magnetic layers. The in-plane component is negligible compared to the external field, and the out-of-plane component is the same for both magnetic layers.

In conclusion, the current dependence of the IL-DMI in SAFs has been found by studying the switching fields obtained from AHE measurements and quantified by means of the resulting IL-DMI field $H_{\mathrm{IL-DMI}}$, which exhibits a significant shift in the azimuthal dependence

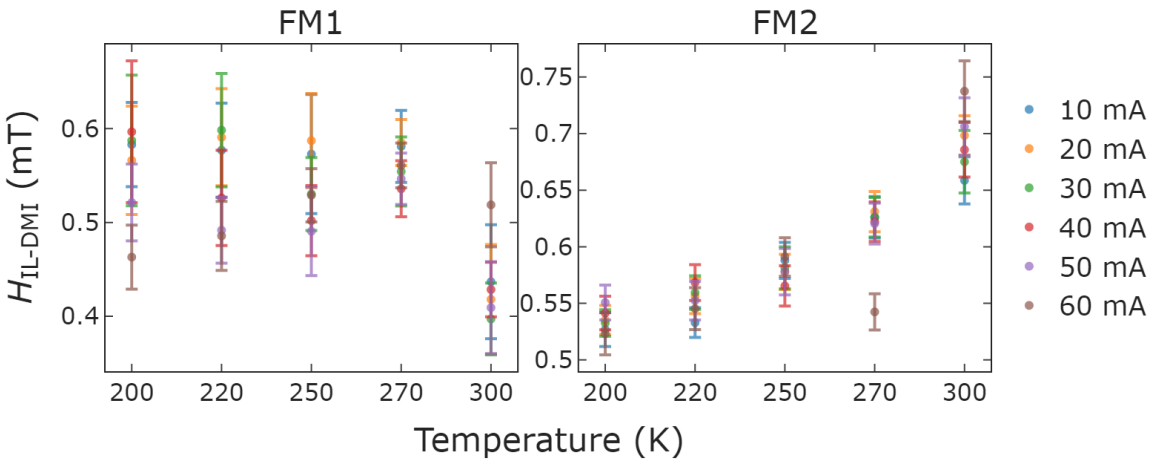

Figure 4: **Temperature dependence.** The IL-DMI field as function of temperature for a continuous film of Ta(4)/Pt(4)/Co(0.6)/Pt(0.5)/Ru(0.8)/Pt(0.5)/Co(1)/Pt(4) measured at various total currents.

for increasing current density. By employing a simple model of two superimposed cosine functions with a static and current-induced contribution, the observed behavior was reliably modeled. The fit yields a current-induced contribution for the IL-DMI that scales linearly with current and is symmetric in current. From the symmetry point of view, an applied electric current along the direction $(\boldsymbol{M}_1 \times \boldsymbol{M}_2) \times \boldsymbol{R}$ – where $\boldsymbol{R}$ is the distance vector between the magnetizations $\boldsymbol{M}_1$ and $\boldsymbol{M}_2$ of the two layers – allows for stabilizing a chiral Néel-type state. A possible mechanism for the current-induced IL-DMI is the spin Hall effect, which provides torques of opposite sign on the two magnetizations FM1 and FM2. While the observed effect is conforming with the performed symmetry analysis, a quantitative theoretical description is still an outstanding task, which is open even for the growth-induced IL-DMI, as minute details on the interfaces or structure of a specific sample need to be correctly addressed. The observed effect appears to be purely current-induced, as growth-induced and current-induced IL-DMI simply superimpose with no apparent mixing term. Therefore, we assume this effect to be present also in systems without growth-induced IL-DMI. Such a current-induced contribution to the IL-DMI allows for the highly desirable control of this chiral interaction

and enables a direct, post-growth tuning mechanism for 3D topological spin structures in future spintronic devices. Notably, the magnitude of the current-induced IL-DMI is found to be similar to the magnitudes so far observed in static IL-DMI already at experimentally manageable dc current densities. Using short current pulses much stronger effects will be available to manipulate 3D spin structures. The current-induced IL-DMI also opens new possibilities for pure-electrical field-free switching. As field-free switching has been observed in samples with IL-DMI,[15,16] it is up to further studies to investigate the relation between current-induced IL-DMI and field-free switching.

Methods

Sample preparation and measurement of the anomalous Hall effect

The magnetic multilayer samples were grown on thermally oxidized Si/SiO_2 wafers with 100 nm oxide thickness employing an ultrahigh-vacuum d.c. magnetron sputtering system with a base pressure of 9.5×10^{-8} mbar and a working pressure of 2×10^{-2} mbar. The samples were grown at room temperature. Sample 1: Ta(4)/Pt(4)/Co(0.6)/Pt(0.7)/Ru(0.8)/Pt(0.5)/Co(1)/Pt(4). Sample 2: Ta(4)/Pt(4)/Co(0.6)/Pt(0.5)/Ru(0.8)/Pt(0.5)/Co(1)/Pt(4). The Ru layer of both samples was sputtered without wafer rotation at off-normal incidence to break the in-plane rotational symmetry. Sample 1 was patterned into Hall bars using electron-beam lithography and subsequent ion-beam etching. The hysteresis loops of the magnetic multilayers are measured by the anomalous Hall signal on a Hall-bar structure for the patterned sample (see Fig. 1a)) and by the van-der-Pauw method for the continuous film. The measurements were performed by sweeping the out-of-plane field while applying a constant in-plane field of 100 mT along varied directions. The transport measurement is performed by applying a constant current. Switching fields are determined by fitting error functions to the jumps in the hysteresis data, with each loop 5 repeated times. Mean and standard error of the switching fields are

calculated for subsequent analysis.

Acknowledgement

F.K. acknowledges funding by the Deutsche Forschungsgemeinschaft (DFG, German Research Foundation) - TRR 173/2 - 268565370 Spin+X (Projects A01 and B02) and the priority program 2137 Skyrmionics (#403502522). The authors acknowledge funding from TopDyn. This project has received funding from the European Research Council (ERC) under the European Union's Horizon 2020 research and innovation programme (Grant No. 856538, project "3D MAGiC"). Y.M. and F.F. acknowledge funding by DFG via TRR 288 - 422213477 (project B06) and - TRR 173/2 - 268565370 Spin+X (Projects A11). F.F. acknowledges funding from the Sino-German research project DISTOMAT (DFG project MO 1731/10-1). K.L. acknowledges the support from the National Research Foundation of Korea (NRF) funded by the Ministry of Science and ICT (2022R1C1C1008604). This work was supported by the National Research Foundation of Korea (NRF) funded by the Korean Government (MSIP) (Grant No. 2020R1C1C1012664, 2020M3F3A2A01081635, 2022M3I7A2079267) and the KIST institutional programs (2E32251, 2E32252).

Supporting Information Available

- Complementary measurements, Simulation of the Oersted field and qualitative discussion of spin-Hall-effect torques.
- The data sets generated and/or analysed during the study will are available from the corresponding author upon reasonable request.

References

(1) López-Ortega, A.; Estrader, M.; Salazar-Alvarez, G.; Roca, A. G.; Nogués, J. Applications of exchange coupled bi-magnetic hard/soft and soft/hard magnetic core/shell nanoparticles. *Physics Reports* **2015**, *553*, 1–32.

(2) Streubel, R.; Kronast, F.; Fischer, P.; Parkinson, D.; Schmidt, O. G.; Makarov, D. Retrieving spin textures on curved magnetic thin films with full-field soft X-ray microscopies. *Nat Commun* **2015**, *6*, 7612.

(3) Fischer, P.; Sanz-Hernández, D.; Streubel, R.; Fernández-Pacheco, A. Launching a new dimension with 3D magnetic nanostructures. *APL Materials* **2020**, *8*, 010701.

(4) Fernández-Pacheco, A.; Streubel, R.; Fruchart, O.; Hertel, R.; Fischer, P.; Cowburn, R. P. Three-dimensional nanomagnetism. *Nature Communications* **2017**, *8*, 15756.

(5) Faddeev, L.; Niemi, A. J. Stable knot-like structures in classical field theory. *Nature* **1997**, *387*, 58–61.

(6) Sutcliffe, P. Hopfions in chiral magnets. *J. Phys. A: Math. Theor.* **2018**, *51*, 375401.

(7) Rybakov, F. N.; Kiselev, N. S.; Borisov, A. B.; Döring, L.; Melcher, C.; Blügel, S. Magnetic Hopfions in Solids. *APL Materials* **2022**, *10*, 111113.

(8) Kent, N.; Reynolds, N.; Raftrey, D.; Campbell, I. T. G.; Virasawmy, S.; Dhuey, S.; Chopdekar, R. V.; Hierro-Rodriguez, A.; Sorrentino, A.; Pereiro, E.; Ferrer, S.; Hellman, F.; Sutcliffe, P.; Fischer, P. Creation and observation of Hopfions in magnetic multilayer systems. *Nature Communications* **2021**, *12*, 1562.

(9) Fert, A.; Cros, V.; Sampaio, J. Skyrmions on the track. *Nature Nanotech* **2013**, *8*, 152–156.

(10) Han, D.-S.; Lee, K.; Hanke, J.-P.; Mokrousov, Y.; Kim, K.-W.; Yoo, W.; Hees, Y. L. W. v.; Kim, T.-W.; Lavrijsen, R.; You, C.-Y.; Swagten, H. J. M.; Jung, M.-H.; Kläui, M. Long-range chiral exchange interaction in synthetic antiferromagnets. *Nature Materials* **2019**, 1.

(11) Fernández-Pacheco, A.; Vedmedenko, E.; Ummelen, F.; Mansell, R.; Petit, D.; Cowburn, R. P. Symmetry-breaking interlayer Dzyaloshinskii–Moriya interactions in synthetic antiferromagnets. *Nature Materials* **2019**, *18*, 679–684.

(12) Vedmedenko, E. Y.; Riego, P.; Arregi, J. A.; Berger, A. Interlayer Dzyaloshinskii-Moriya Interactions. *Phys. Rev. Lett.* **2019**, *122*, 257202.

(13) Avci, C. O.; Lambert, C.-H.; Sala, G.; Gambardella, P. Chiral Coupling between Magnetic Layers with Orthogonal Magnetization. *Phys. Rev. Lett.* **2021**, *127*, 167202.

(14) Guo, Y.; Zhang, J.; Cui, Q.; Liu, R.; Ga, Y.; Zhan, X.; Lyu, H.; Hu, C.; Li, J.; Zhou, J.; Wei, H.; Zhu, T.; Yang, H.; Wang, S. Effect of interlayer Dzyaloshinskii-Moriya interaction on spin structure in synthetic antiferromagnetic multilayers. *Phys. Rev. B* **2022**, *105*, 184405.

(15) Huang, Y.-H.; Huang, C.-C.; Liao, W.-B.; Chen, T.-Y.; Pai, C.-F. Growth-Dependent Interlayer Chiral Exchange and Field-Free Switching. *Phys. Rev. Applied* **2022**, *18*, 034046.

(16) He, W.; Wan, C.; Zheng, C.; Wang, Y.; Wang, X.; Ma, T.; Wang, Y.; Guo, C.; Luo, X.; Stebliy, M. E.; Yu, G.; Liu, Y.; Ognev, A. V.; Samardak, A. S.; Han, X. Field-Free Spin–Orbit Torque Switching Enabled by the Interlayer Dzyaloshinskii–Moriya Interaction. *Nano Lett.* **2022**, *22*, 6857–6865.

(17) Liu, Y.; Hou, W.; Han, X.; Zang, J. Three-Dimensional Dynamics of a Magnetic Hopfion Driven by Spin Transfer Torque. *Phys. Rev. Lett.* **2020**, *124*, 127204.

(18) Han, D.-S.; Lee, K.; Hanke, J.-P.; Mokrousov, Y.; Kim, K.-W.; Yoo, W.; van Hees, Y. L. W.; Kim, T.-W.; Lavrijsen, R.; You, C.-Y.; Swagten, H. J. M.; Jung, M.-H.; Kläui, M. Long-range chiral exchange interaction in synthetic antiferromagnets. *Nat. Mater.* **2019**, *18*, 703–708.

(19) Deger, C. Strain-enhanced Dzyaloshinskii–Moriya interaction at Co/Pt interfaces. *Sci Rep* **2020**, *10*, 12314.

(20) Filianina, M. Electric field-induced strain control of magnetism in in-plane and out-of-plane magnetized thin films. PhD Thesis, Johannes Gutenberg-Universität Mainz, Mainz, 2021.

(21) Shen, Z.; Song, C.; Xue, Y.; Wu, Z.; Wang, J.; Zhong, Z. Strain-Tunable Dzyaloshinskii-Moriya Interaction and Skyrmions in Two-Dimensional Janus $Cr_2\{X_3Y_3$ (X, Y = Cl, Br, I, $X \neq Y$) Trihalide Monolayers. *Physical Review B* **2022**, *106*, 094403.

(22) Hirsch, J. E. Spin Hall Effect. *Phys. Rev. Lett.* **1999**, *83*, 1834–1837.

(23) Miron, I. M.; Garello, K.; Gaudin, G.; Zermatten, P.-J.; Costache, M. V.; Auffret, S.; Bandiera, S.; Rodmacq, B.; Schuhl, A.; Gambardella, P. Perpendicular switching of a single ferromagnetic layer induced by in-plane current injection. *Nature* **2011**, *476*, 189–193.

(24) Emori, S.; Bauer, U.; Ahn, S.-M.; Martinez, E.; Beach, G. S. D. Current-driven dynamics of chiral ferromagnetic domain walls. *Nature Materials* **2013**, *12*, 611–616.

(25) Manchon, A.; ıfmmode \checkZ\else Ž\fielezný, J.; Miron, I. M.; Jungwirth, T.; Sinova, J.; Thiaville, A.; Garello, K.; Gambardella, P. Current-induced spin-orbit torques in ferromagnetic and antiferromagnetic systems. *Rev. Mod. Phys.* **2019**, *91*, 035004.

(26) Karnad, G.; Freimuth, F.; Martinez, E.; Lo Conte, R.; Gubbiotti, G.; Schulz, T.; Senz, S.; Ocker, B.; Mokrousov, Y.; Kläui, M. Modification of Dzyaloshinskii-Moriya-Interaction-Stabilized Domain Wall Chirality by Driving Currents. *Phys. Rev. Lett.* **2018**, *121*, 147203.

(27) Kato, N.; Kawaguchi, M.; Lau, Y.-C.; Kikuchi, T.; Nakatani, Y.; Hayashi, M. Current-Induced Modulation of the Interfacial Dzyaloshinskii-Moriya Interaction. *Phys. Rev. Lett.* **2019**, *122*, 257205.

(28) Freimuth, F.; Blügel, S.; Mokrousov, Y. Dynamical and current-induced Dzyaloshinskii-Moriya interaction: Role for damping, gyromagnetism, and current-induced torques in noncollinear magnets. *Phys. Rev. B* **2020**, *102*, 245411.

(29) Kikuchi, T.; Koretsune, T.; Arita, R.; Tatara, G. Dzyaloshinskii-Moriya Interaction as a Consequence of a Doppler Shift due to Spin-Orbit-Induced Intrinsic Spin Current. *Phys. Rev. Lett.* **2016**, *116*, 247201.

(30) Freimuth, F.; Blügel, S.; Mokrousov, Y. Relation of the Dzyaloshinskii-Moriya interaction to spin currents and to the spin-orbit field. *Phys. Rev. B* **2017**, *96*, 054403.

(31) Han, D.-S.; Kim, N.-H.; Kim, J.-S.; Yin, Y.; Koo, J.-W.; Cho, J.; Lee, S.; Kläui, M.; Swagten, H. J. M.; Koopmans, B.; You, C.-Y. Asymmetric Hysteresis for Probing Dzyaloshinskii–Moriya Interaction. *Nano Lett.* **2016**, *16*, 4438–4446.

(32) Stamps, R. L. Mechanisms for exchange bias. *J. Phys. D: Appl. Phys.* **2000**, *33*, R247–R268.

(33) Meiklejohn, W. H.; Bean, C. P. New Magnetic Anisotropy. *Phys. Rev.* **1957**, *105*, 904–913.

(34) Slonczewski, J. C. Origin of biquadratic exchange in magnetic multilayers (invited). *Journal of Applied Physics* **1993**, *73*, 5957–5962.

(35) Slonczewski, J. C. Fluctuation mechanism for biquadratic exchange coupling in magnetic multilayers. *Phys. Rev. Lett.* **1991**, *67*, 3172–3175.

(36) Meer, H.; Schreiber, F.; Schmitt, C.; Ramos, R.; Saitoh, E.; Gomonay, O.; Sinova, J.; Baldrati, L.; Kläui, M. Direct Imaging of Current-Induced Antiferromagnetic Switching Revealing a Pure Thermomagnetoelastic Switching Mechanism in NiO. *Nano Lett.* **2021**, *21*, 114–119.